Volume 1 | Number 1 | Jan 2013 | Pages 1–100

ChemComm

Chemical Communications
www.rsc.org/chemcomm

ROYAL SOCIETY OF CHEMISTRY

This is an *Accepted Manuscript*, which has been through the Royal Society of Chemistry peer review process and has been accepted for publication.

Accepted Manuscripts are published online shortly after acceptance, before technical editing, formatting and proof reading. Using this free service, authors can make their results available to the community, in citable form, before we publish the edited article. We will replace this *Accepted Manuscript* with the edited and formatted *Advance Article* as soon as it is available.

You can find more information about *Accepted Manuscripts* in the **Information for Authors**.

Please note that technical editing may introduce minor changes to the text and/or graphics, which may alter content. The journal's standard **Terms & Conditions** and the **Ethical guidelines** still apply. In no event shall the Royal Society of Chemistry be held responsible for any errors or omissions in this *Accepted Manuscript* or any consequences arising from the use of any information it contains.

www.rsc.org/chemcomm

ChemComm

COMMUNICATION

High alkalinity boosts visible light driven H$_2$ evolution activity of g-C$_3$N$_4$ in aqueous methanol

Po Wu,[a,b] Jiarui Wang,[b] Jing Zhao,[b] Liejin Guo*[a] and Frank E. Osterloh*[b]

A high rate of 2.23 mmol·h^{-1}·g^{-1} (quantum efficiency of 6.67% at 400 nm) for visible light driven photocatalytic H$_2$ evolution can be achieved with g-C$_3$N$_4$ by alkalization of the solution to a pH of 13.3, due to accelerated transfer of photoholes to the sacrificial donor.

Hydrogen production from photocatalytic water splitting under sunlight is regarded as a possible solution to the global energy and environmental problems resulting from fossil fuel consumption.[1] However, the design of efficient visible-light-responsive photocatalysts remains a great challenge.[2] Different from the widely studied inorganic semiconductors (mainly oxides),[3] graphitic carbon nitride (g-C$_3$N$_4$) has aroused great interest in recent years, due to the appropriate band edge potentials and ease of synthesis.[4] However, the efficiency of the material is limited by high recombination rate. Improved hydrogen evolution rate (HER) can be achieved by increasing the surface area in porous [5] or nanosheet [6] forms of g-C$_3$N$_4$, or by introducing internal junctions to promote charge separation.[7] Herein, we report that the solution pH is a significant factor for the HER of g-C$_3$N$_4$. High alkalinity boosts hydrogen evolution to 2.23 mmol·h^{-1}·g^{-1} under visible light and allows for a quantum efficiency of 6.67% (400 nm). These values exceed those previously reported for g-C$_3$N$_4$.[8-10] Based on electrochemical and photovoltage data, the high activity is a result of an increased thermodynamic driving force for hole transfer at high pH.

The g-C$_3$N$_4$ materials used for this study were synthesised by heating either dicyandiamide (D), urea (U), thiourea (T) or stoichiometric mixtures (UT, 1:1 weight ratio) at 520 °C, to yield D52, U52, T52 and UT52, respectively. X-ray diffraction (XRD) patterns and Fourier transform infrared (FTIR) spectra (Fig. S1 and S2) agree with the literature data,[4, 11] confirming the graphitic structure. Fig. 1 shows an absorption edge at about 450 nm for all the samples. The corresponding bandgap values can be obtained by the intercept of extended linear region in the Tauc

plot (right inset).[12] They vary from 2.88 eV for D52 to 2.99 eV for U52. U52 has the largest band gap, which may be a result of quantum confinement.[13] This is supported by a longer interlayer distance revealed from the low-angle shifted XRD patterns of the material (Fig. S1). For T52 and UT52, the absorption spectra show a shoulder extending to 600 nm, indicative of the presence of defects in the band gap. In accord with this, the yellow colour of these materials is slightly darker.
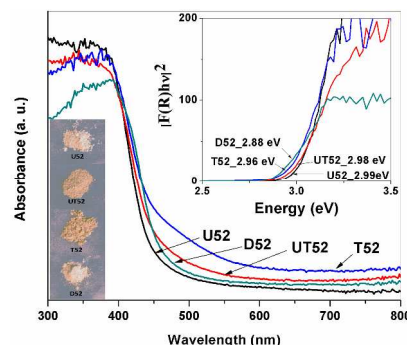

Fig. 1. UV-Vis absorption spectra, photos (left inset) and Tauc plots (right inset) of samples U52, UT52, T52 and D52.

In order to determine the photocatalytic hydrogen evolution activity of the materials, 1% (mass) of platinum was photodeposited on each sample. The visible light H$_2$ evolution from the resulting materials in aqueous methanol at pH 4.5 is shown in Fig. 2A. D52 had a better performance than U52 and T52, owing to less defects and better crystallization (Fig. S1). UT52 presented a reaction rate of ca. 762 µmol·h^{-1}·g^{-1}, which is over four times higher than that of U52 and T52. It should be noted that, UT52 had less absorption than T52 (Fig. 1), but it had a significantly improved H$_2$ evolution activity, indicating that light absorption does not play the most important role in this photocatalytic reaction over g-C$_3$N$_4$. According to earlier studies, the enhanced performance of UT52 is attributed to a

heterojunction in this material,[7] which arises from the use of two separate synthetic precursors, urea and thiourea. The compositional variations within the mixed g-C_3N_4 product generate a 0.1 eV conduction band (CB) offset and a 0.4 eV valence band (VB) offset that facilitate charge separation inside the material.[14] Our TEM images (Fig. S3) seem to support this interpretation. They show a porous morphology for U52, a compact morphology for T52, and a combination of both for UT52.
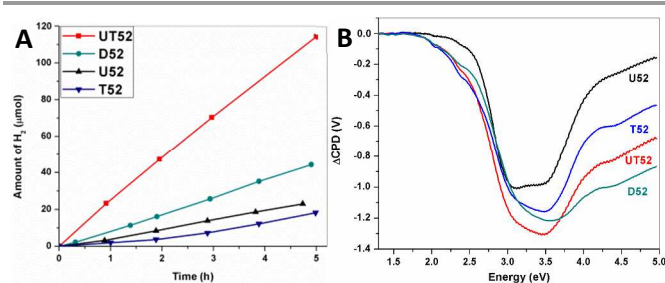

Fig. 2. A) H_2 evolution from the samples (30 mg) in methanol (20 vol. %) aqueous solution at pH=4.5 under visible-light (λ > 400 nm) irradiation. The light power at the flask surface was 380 mW/cm². Samples were platinized with Pt (1 w. %) by photodeposition prior to testing. B) SPV spectra of samples U52, UT52, T52 and D52. Films had average thickness of ca. 5 μm.

To investigate the charge separation in g-C_3N_4, surface photovoltage (SPV) spectra were recorded for the entire series. In SPV, the surface potential of an illuminated particle film is measured as a function of photon energy.[15-17] The observed contact potential variations (ΔCPD) provide information about the majority carrier type, band gap, and other properties of the light absorber.[18-20] Measured spectra are shown in Fig. 2B. In all cases, negative voltages are observed, indicating majority carrier (electron) transfer from g-C_3N_4 into the ITO substrate. Small sub-gap photovoltage signals in particular for UT52/T52 and D52 can be attributed to defects, which is consistent with the UV-Vis spectra. The maximum photovoltage for these samples occur around 3.0-3.5 eV. Values lie between 1.01 V and 1.31 V, with the highest value observed for UT52. This suggests that charge separation and carrier lifetimes are improved in this material.

Recently, it has been reported that hydrogen evolution over SrTiO₃ could be improved significantly in alkaline solution.[21] To determine if a similar pH-dependence exists for g-C_3N_4, illumination experiments for D52 were carried out at variable pH conditions. D52 was chosen because it is the most common form of g-C_3N_4 described in the literature. As shown in Fig. 3A, steady H_2 evolution is observed in all cases, with the evolution rate rising continuously as the pH value is increased. The highest activity is 1.56 mmol·h⁻¹·g⁻¹ at pH=13.3. The enhanced activity is not temporary but persistent for at least 15 h (Fig. S4), yielding a turnover number of 1.82 based on 594 μmol evolved H_2. When the rates are plotted versus pH (Fig. 3B), a nearly exponential dependence between pH and the reaction rate is observed.

To rule out ionic strength as a factor, control experiments were conducted with KCl and NaOH electrolytes (Fig. 3C). These experiments show that KCl does not improve the reaction rate, whereas KOH yields four times higher activity. This rate improvement is comparable to NaOH, which shows that

hydroxide concentration is the key parameter. A further boost of the activity could be achieved by replacing D52 with UT52. At pH=13.3, the H_2 evolution rate is 2.23 mmol·h⁻¹·g⁻¹, approximately 14 times higher than that of U52 at pH 4.5. To determine the AQY, H_2 evolution was performed under LED illumination (400 nm). From the rates in Fig. 3D, the AQY of D52 and UT52 were calculated to be ca. 3.84% and 6.67 %, respectively. To our knowledge, this ranks among the highest activities reported for g-C_3N_4 (1.8%-26.5%).[8, 22] The total amount of H_2 generated over UT52 (1.32 mmol in 2 hours), exceeds the molar amount of g-C_3N_4 (0.33 mmol) by a factor of three, confirming the catalytic nature of the reaction. Additionally, FTIR spectra recorded for g-C_3N_4 before and after the reaction (Fig. S5) do not show any photocatalyst degradation.
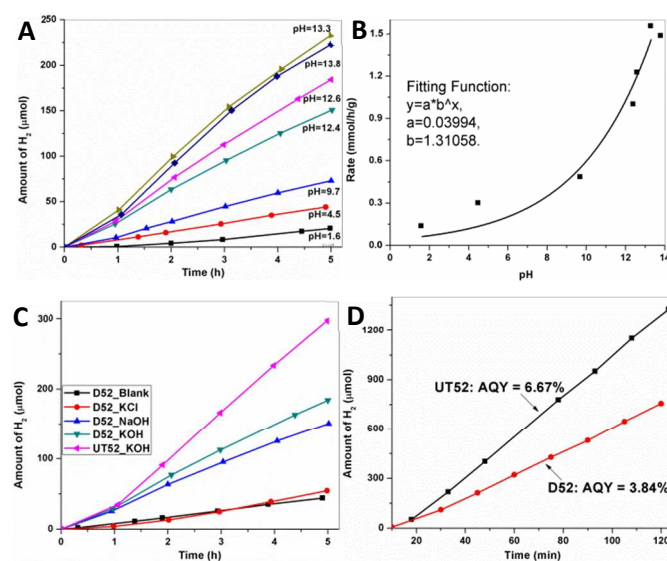

Fig. 3. A) H_2 evolution from from D52 (30 mg) in methanol (20 vol. %) aqueous solution at different pH under visible light (λ > 400 nm) irradiation. B) Plot of H_2 evolution rate vs. pH from A) and the fitted exponential curve. C) H_2 evolution in the presence of various electrolytes (0.4 M). D) H_2 evolution over D52 or UT52 (30 mg) in basic (pH=13.3) methanol (20 vol. %) aqueous solution under 400 nm LED light irradiation for AQY calculation.

To elucidate the reasons for the increased activity, photocurrent scans were recorded on g-C_3N_4 films immersed in neutral or basic electrolyte solution, with or without added methanol (Fig. 4A and S6). Under constant applied bias of 1.20 V (vs. RHE), a g-C_3N_4 film made of D52 only exhibits small chopped photocurrents of ca. 0.6 μA·cm⁻². Upon addition of methanol the photocurrent increases to 1.2 μA·cm⁻², and an additional increase to 4.2 μA·cm⁻² occurs after the addition of base to bring the pH to 12.8. This shows that hole transfer into the solution is promoted by the addition of methanol, especially at high pH. Photocurrent scans versus applied potential are shown in Fig. 4B. In 0.2 M Na₂SO₄ solution at pH=5.6 (acidity due to CO₂ from air), a g-C_3N_4 film produces weak cathodic and anodic photocurrents when the applied potential was negative or positive of +0.38 V (vs. NHE). These currents are limited by slow charge transport in the g-C_3N_4 film, and by the absence of a space charge layer that could provide a photovoltage. When methanol (12.5 vol. %) was added to the electrolyte, the cathodic

photocurrent was suppressed and the anodic photocurrent was increased by 300%. This shows that methanol speeds up hole transfer from g-C_3N_4. Under these conditions the anodic photo-onset potential can be taken as the quasi-Fermi level ($E_{F,n}$) of g-C_3N_4. The onset at +0.03 V (vs. NHE) is more negative than that without methanol (+0.38 V vs. NHE), in agreement with faster hole removal from g-C_3N_4, which reduces the positive charging of the material. The g-C_3N_4 flat-band and band-edge potentials, together with the methanol (and proton) redox potential, are shown in Fig. 4D.
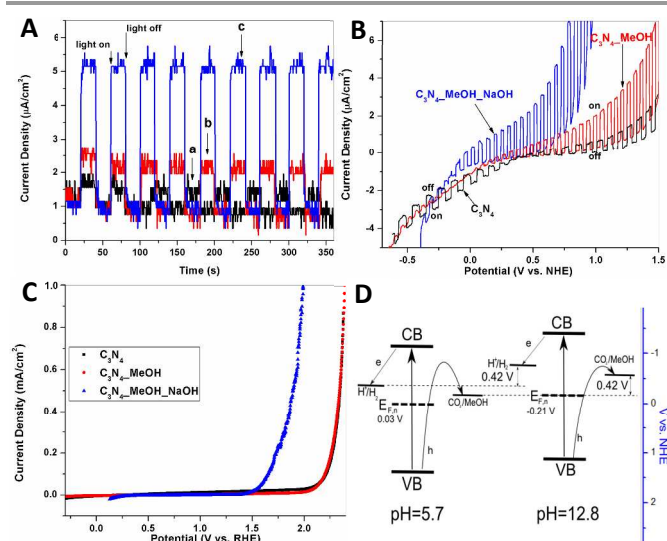

Fig. 4. A) Photocurrent at 1.20 V (vs. RHE) for g-C_3N_4 film in aqueous NaOH solution (pH=5.6, 5.7 and 12.8 for D52 [a], D52/MeOH [b] and D52/MeOH/NaOH [c], respectively) with or without 12.5 vol. % methanol. A fiberoptics Xe light source (60 mWcm^{-2} at electrode) was used. B) Photocurrent scans (positive to negative potential, 20 mV·s^{-1}), C) Dark current scans in different solutions. D) Energy diagrams of g-C_3N_4 at neutral and basic solution. 'The slightly lower pH (12.8) was used in the electrochemical experiments in order to prevent corrosion of the reference electrode at high pH.'

Several changes in the system energetics occur upon raising the solution from 5.7 to 12.8 with NaOH. First, dark electrochemical scans on a g-C_3N_4 film electrode in aqueous methanol (Fig. 4C) show that the CH_3OH oxidation potential shifts cathodically by 0.54 V (vs. RHE) when the pH increases. Indeed, it is known that hydroxide facilitates proton abstraction from CH_3OH and promotes oxidation.[23] This pH change is expected to also move the quasi-Fermi level in g-C_3N_4 to more reducing values. However, the observed shift in the photoelectrochemical onset potential (Fig. 4B) from +0.03 V to -0.21 V (vs. NHE) is only 0.24 V, i.e. -0.032 per pH unit. This sub-Nernstian shift [24] can be explained by the acid-base chemistry of g-C_3N_4. It is well known that the surface of g-C_3N_4 is terminated by -NH/NH_2 groups [25] whose acidity is much lower than that of -OH typically found on the surface of metal oxides (pK$_a$ =38 for NH_3; pK$_a$ =14 for H_2O).[26, 27] As a result, no significant deprotonation occurs at pH=12.8, explaining the lack of negative charging and the sub-Nernstian Fermi level shift. This results in an increased driving force of 0.18 eV for hole transfer from g-C_3N_4 to methanol (Fig. 4D), and correspondingly higher charge transfer rate. This effect explains the higher photocatalytic hydrogen evolution rate resulting from

alkalization. While the HER boost formally resembles that for photocatalytic hydrogen evolution from $SrTiO_3$,[21] the reason is fundamentally different. In the latter case, the enhancement at high pH is attributed to the generation of reactive hydroxyl radicals from hydroxide. This mechanism can be ruled out for g-C_3N_4 because the material does not contain significant hydroxide groups on the surface. The model also provides a simple explanation for the high photocatalytic HER reported by Martin et al.[22] In that system, H_2 evolution tests were performed in 13% (v:v) triethanolamine solution in water. The pH of this solution was not stated in the paper but can be estimated as pH = 10.9, based on the pk$_b$ = 6.24 for triethanolamine. That pH is close to the conditions employed here, and suggests the presence of a significant pH effect in that system.

Conclusions

In summary, we demonstrate a significant boost for the photocatalytic hydrogen evolution activity of g-C_3N_4 in solutions of sacrificial electron donors. In the case of UT52, high pH enable record HER activity (2.23 mmol·h^{-1}·g^{-1}, AQY 6.67% at 400 nm) under visible light. The mechanism for this enhancement is revealed on the basis of surface photovoltage spectra and electrochemical measurements. It is mainly due to the increased driving force for photochemical methanol oxidation at high pH, which stems from the low acidity of the amine terminated g-C_3N_4 surface. This mechanism also explains the high activity for g-C_3N_4 in triethanolamine solution. Overall, this work promotes the understanding of photochemical charge transfer at non-oxide surfaces, as relevant to the conversion of sunlight into fuel.

Notes and references

[a] International Research Center for Renewable Energy, State Key Laboratory of Multiphase Flow in Power Engineering, Xi'an Jiaotong University, No.28 West Xianning Road, Xi'an, Shaanxi, 710049, P.R.China. Tel:(+86)02982663895; Fax: (+86)02982669033; E-mail: lj-guo@mail.xjtu.edu.cn.
[b] Department of Chemistry, University of California, Davis. One Shields Avenue, Davis, CA, 95616, USA. Tel: (+1)5307546242; E-mail: fosterloh@ucdavis.edu

† Electronic Supplementary Information (ESI) available: Experimental details and Fig. S1-S7. See DOI: 10.1039/c000000x/

1. F. E. Osterloh., *Chem. Soc. Rev.*, 2013, **42** 2294.
2. X. B. Chen, S. H. Shen, L. J. Guo and S. S. Mao, *Chem. Rev.*, 2010, **110**, 6503.
3. F. E. Osterloh, *Chem. Mater.*, 2008, **20**, 35.
4. X. Wang, K. Maeda, A. Thomas, K. Takanabe, G. Xin, J. M. Carlsson, K. Domen and M. Antonietti, *Nat. Mater.*, 2009, **8**, 76.
5. Y. Wang, X. Wang and M. Antonietti, *Angew. Chem. Int. Edit*, 2012, **51**, 68.

6. X. Zhang, X. Xie, H. Wang, J. Zhang, B. Pan and Y. Xie, *J. Am. Chem. Soc.*, 2013, **135**, 18.
7. F. Dong, Z. Zhao, T. Xiong, Z. Ni, W. Zhang, Y. Sun and W.-K. Ho, *ACS Appl. Mater. Inter.*, 2013, **5**, 11392.
8. H. Yan, *Chem. Commun.*, 2012, **48**, 3430.
9. J. Hong, X. Xia, Y. Wang and R. Xu, *J. Mater. Chem.*, 2012, **22**, 15006.
10. Y.-S. Jun, J. Park, S. U. Lee, A. Thomas, W. H. Hong and G. D. Stucky, *Angew. Chem.*, 2013, **125**, 11289.
11. S. Martha, A. Nashim and K. M. Parida, *J. Mater. Chem. A*, 2013, **1**, 7816.
12. S. Datta and K. L. Narasimhan, *Phys. Rev. B*, 1999, **60**, 8246.
13. A. P. Alivisatos, *Science*, 1996, **271**, 933.
14. J. Chen, S. Shen, P. Guo, M. Wang, P. Wu, X. Wang and L. Guo, *Appl. Catal. B-Environ*, 2014, **152**, 335.
15. L. Kronik and Y. Shapira, *Surf. Interface Anal.*, 2001, **31**, 954.
16. L. Kronik and Y. Shapira, *Surf. Sci. Rep.*, 1999, **37**, 1.
17. J. Lagowski, *Surf. Sci.* , 1994, **299**, 92.
18. J. Zhao and F. E. Osterloh, *J. Phys. Chem. Lett.*, 2014, **5**, 782.
19. F. E. Osterloh, M. A. Holmes, J. Zhao, L. Chang, S. Kawula, J. D. Roehling and A. J. Moulé, *J. Phys. Chem. C*, 2014, **118**, 14723.
20. F. E. Osterloh, M. A. Holmes, L. Chang, A. J. Moulé and J. Zhao, *J. Phys. Chem. C*, 2013, **117**, 26905.
21. S. Ouyang, H. Tong, N. Umezawa, J. Cao, P. Li, Y. Bi, Y. Zhang and J. Ye, *J. Am. Chem. Soc.*, 2012, **134**, 1974.
22. D. J. Martin, K. Qiu, S. A. Shevlin, A. D. Handoko, X. Chen, Z. Guo and J. Tang, *Angew. Chem. Int. Ed.*, 2014, **53**, 9240.
23. J. Prabhuram and R. Manoharan, *J. Power Sources*, 1998, **74**, 54.
24. R. L. Chamousis and F. E. Osterloh, *Energy Environ. Sci.*, 2014, **7**, 736.
25. J. A. Singh, S. H. Overbury, N. J. Dudney, M. Li and G. M. Veith, *ACS Catal.*, 2012, **2**, 1138.
26. D. D. Perrin, in *CRC Handbook of Chemistry and Physics*, CRC Press/Taylor and Francis, Boca Raton, FL, 2008.
27. E. Buncel and B. Menon, *J. Organomet. Chem.*, 1977, **141**, 1.

ChemComm Accepted Manuscript